Engineering of Calcium Alginate- PANI@Sawdust Wood hydrogel Bio-beads for the Removal of the Sulfonate Groups-Containing Orange G dye from Aqueous Solution

ABDELAZIZ IMGHARN (abdelaziz.imgharn@edu.uiz.ac.ma)
Ibn Zohr University: Universite Ibn Zohr

Nouh Aarab
Ibn Zohr University: Universite Ibn Zohr

Abdelghani Hsini
Ibn Zohr University: Universite Ibn Zohr

Yassine Naciri
Ibn Zohr University: Universite Ibn Zohr

Mohammed Elhoudi
Ibn Zohr University: Universite Ibn Zohr

Mohamed Ait Haki
Ibn Zohr University: Universite Ibn Zohr

Mohamed Laabd
Ibn Zohr University: Universite Ibn Zohr

Rajae Lakhmiri
Abdelmalek Essaadi University: Universite Abdelmalek Essaadi

Abdallah Albourine
Ibn Zohr University: Universite Ibn Zohr

Research Article

Keywords: Calcium alginate, PANI@SD, sawdust wood, biobeads, OG dye removal

Posted Date: December 10th, 2021

DOI: https://doi.org/10.21203/rs.3.rs-979902/v1

Abstract

The aim of this work is to investigate the adsorption performance of orange G (OG) dye from aqueous solutions employing PANI@sawdust biocomposite enrobed by calcium-alginate biobeads (Alg-PANI@SD). The as-prepared adsorbent was characterized by scanning-electron-microscopy (SEM), X-ray energy dispersive spectroscopy (EDS) and Fourier transforms infrared (FT-IR) spectroscopy, and used to remove Orange G dye from water. batch tests were performed as a function of adsorbent dosage, pH, contact time, interfering ions and initial OG dye concentration. Experimental results show that the kinetic model of pseudo-first-order (PFO) and Freundlich isotherm provided a good fitting of the whole experimental data. The results revealed that the as-prepared tricomposite Alg-PANI@SD, has the potential to be applied as a low-cost adsorbent for the adsorption of OG dye from aqueous media.

1. Introduction

The rapid influx of people growing creates a clean-water challenge, that is already being confronted in the world (Chang et al. 2016; Pradhan et al. 2020). The water pollution threat could be caused by industry such as the release of dyes into the environment in the form of wastewater (Salam et al. 2017; Yeamin et al. 2021). The occurrence of dyes, even at low concentrations, in water adversely affects human health and is toxic to the life of microorganisms and their biological systems (Zheng et al. 2019). Various dyes resist biodegradation due to their aromatic structure. Among the dyes, Orange G (OG) is generally used in textile tanneries. OG dye is one of the azo dyes and could be cause irritation to the skin, eyes and mucous membranes, respiratory organs and cancer (Imgharn et al. 2021). Therefore, the elimination of dyes from contaminated water is necessary before their release into the natural environment. For this purpose, several techniques have been developed, such as chemical precipitation (Singh and Chauhan 2009), photodegradation processes (Miklos et al. 2018; Naciri et al. 2021), coagulation-flocculation (El-Gaayda et al. 2021), ion exchange and adsorption processes (Grzegorzek et al. 2020; Laabd et al. 2021; Hsini et al. 2021b). The superiority of adsorption separating pollutants owing to the flexibility in design and system, and good output performance in several cases, the capability to reuse the adsorbent in several times, and the low cost of process (Hsini et al. 2021a; Laabd et al. 2021) .

A large collection of biosorbents or biomaterials from natural sources like almond shells, walnut shells, bagasse sugarcane, sawdust, and biomass made up of living, or dead microorganisms, and biopolymers were employed as adsorbents to adsorb contaminants from aqueous solutions, owing of their low cost, availability and their adsorption capacity to treat wastewater (Hsini et al. 2020). However, all these materials provide a simple uptake of contaminants. In order to anhance the adsorption performance of biomaterials, conducting polymers have been increasingly used for their adsorption capability and the polyaniline (PANI) is the most efficient among them (Laabd et al. 2022). Because of its porous structure, regenerability and ion exchange capacity, as well as a large number of amine/imine groups.

Polysaccharide alginate is commonly obtained from brown seaweed. As a biopolymer, sodium alginate is largely applied in pharmaceuticals, cosmetic and hygienic products, textiles, food additives and dyes

(Rocher et al. 2008). This polymer has very long-chain molecules with active carboxylic groups that can be straightened along with each other in a way to be in line with the capability to create a leaf material. One of the tunable qualities of alginate is the capacity to build a hydrogel (Dąbrowski et al. 2005; Javanbakht and Shafiei 2020). An aqueous alginate solution is easily crystallized into a hydrogel, plus double metal cations such as Ca^{2+}.

The main purpose of the current work is to the encapsulation of PANI@SD biocomposite in calcium alginate biobeads as a new eco-friendly adsorbent for OG dye adsorption from aqueous media. The engineered biobeads were characterized by SEM, EDX and FT-IR analyses. Batch testts were carried out for Orange G molecules removal experiments using the prepared biobeads. The effect of contact time, adsorbent doses, pH, initial OG dye concentration, and the co-interfernig ions, kinetics, isotherm studies were evaluated.

2. Materials And Method

2.1. Engineering of Alginate-PANI@SD biobeads

The Sawdust was washed and then air-dried for 4 days. The dried sawdust was crushed and sieved. This SD powder was washed with distilled water and then dried in an oven at 80°C for 24h.

PANI composite was synthesized applying in situ polymerization of aniline monomer in the occurrence of SD particles (Imgharn et al. 2021). In a typical procedure, 1g of SD powder and 1 mL of distilled aniline monomer were added to 80 mL of HCl (1 M). The mix was sonicated for 1 h and the kept under stirring for 3 h. Afterward, sodium persulfate was dissolved in 40 mL of the HCl (1 M) solution and added drop-wise to the suspension under stirring for 6 h at 298K. The resultant precipitate was leached with deionized water and acetone. Finally, the precipitate (PANI@SD) was dried at 80°C overnight.

For the fabrication of the Alg-PANI@SD biobeads, the 1:1 weight ratio of the synthesized PANI@SD biocomposite and sodium alginate was added to 50 ml distilled water and kept under stirring for 3 h until the formation of a viscose gel. In order to form the biobeads, we added dropwise using a syringe with a 4 cm distance between the needle and the solution surface, the gel to the solution of 0.5 M calcium chloride 0.5 M as cross-linker. The prepared alginate-PANI@SD biobeads were stirred for 30 min, then the final biobeads were washed with distilled water.

2.2. Characterization of Alg-PANI@SD biobeads

Morphological analysis was analyzed by scanning electron microscopy (SEM, JEOL, JSM-IT200) coupled energy dispersive spectroscopy (EDS). Fourier-transform infrared (FTIR) spectra of the obtained samples were documented on KBr pellets using FT-IR spectroscopy (ALPHA-Bruker Optics, Germany) wavenumber range from 400 to 4000 cm^{-1}.

The point zero of charge (pH_{PZC}) was defined by a conventional technique, which involves preparing 60 ml solutions of KNO_3 (0.03 M) and modifying their pH to accurate values (2 – 10). Next, 0.45 g of biobeads were added to every solution. The mix was kept under stirring at ambient temperature for 24 h before calculating the pH_{final}. The pH_{PZC} was computed from the curve of pH_{final}-pH_{initia}l = $f(pH_{initial})$.

2.3. Batch experimental studies

In a series of 100 ml beakers, 50 ml of aqueous solutions of OG with specified concentrations were added into a defined amount of biobeads in order to conduct the adsorption measurements. The mix was stirred at 120 rpm and under a constant temperature of 298K for 180 min. At a fixed time, the stirring was stopped, and the samples were centrifuged. The OG dye residual concentration in the reaction mix was evaluated via UV2300 spectrophotometer. Adsorption tests were performed by changing initial solution pH, contact time, adsorbent dose, co-interfering ions and initial OG concentration for adsorption kinetics and adsorption isotherm.

The adsorbed amount of dye onto the adsorbents at time t is Q_t was determined by the following equation (Shuang et al. 2012; Essekri et al. 2021):

$$R(\%) = \frac{\left(C_0 - C_e\right)}{C_0} \times 100 (1)$$

Furthermore, the dye elimination efficiency, i.e., percent of adsorption, was examined as:

$$Q_e = \frac{\left(C_0 - C_e\right)}{m} \times V (2)$$

C_0 is the initial OG dye concentration (mg/L), C_t is the concentration of OG dye at time t, V is the volume of OG dye containing-solution (L), and m is the mass of adsorbents in g. Experiments at the equilibrium were carried out via the above process with a broad array of initial dye concentration. The time of contact between solid-liquid was 180 min, which was higher than the equilibrium time.

3. Results And Discussion

3.1. Characterization of Alg-PANI@SD biobeads

3.1.1. Texture morphology

SEM investigation associated with EDX was figured out the morphologies and chemical composition of SD, PANI@SD and Alg-PANI@SD biobeads as shown in **Fig. 1 (a-c)**. As shown in **Fig. 1 (a-c)**, the SEM images presente that the SD particle has a heterogeneous and porous texture, while the SEM image of the PANI@SD biocomposite suggests that the sawdust surface has been successfully enrobed by PANI

particles, conducting to the generation of pores within the PANI@SD composite structure. These pores may ease the diffusion of sulfonate groups ($-SO_3Na$)-containing OG molecules into the PANI@SD surface. Therefore, SEM image of the Alg-PANI@SD biobeads depicts that the PANI@SD particles were inside a layer formed by alginate and calcium alginate ions allowing the construction of spherical biobeads.

The elemental compositions obtained from the EDX analysis are presented in **fig. (d-e)**. The EDS analysis spectrum of SD (**Figure 1 (d)**) depicts that the sawdust contains mainly carbon and oxygen elements. Figure III-1 e confirms the occurrence of all the atoms attributing to sawdust (C and O) as well as those of polyaniline polymer like nitrogen (N), and sulfur (S) for PANI@SD biocompsite. Moreover, Alg-PANI@SD biobeads showed the existence of elements corresponding to PANI@SD biobeads with the appearance of the other two elements returning to the alginate/Ca^{2+} complex formed.

3.1.2. FT-IR Analysis

The structural characteristics of sawdust (SD), PANI@SD and Alg-PANI@SD biobeads were figured out employing FTIR spectroscopy technique. The spectra of SD, PANI@SD and Alg-PANI@SD are given in Fig. 2, respectively.

In the spectrum of SD, we notice a band at 3427 cm^{-1} is ascribed to the stretching vibration of O-H groups, the peak centered at 3000 cm^{-1} are owing to the C-H stretching vibrations and specify the occurrence of alkanes. The band at 1721 cm^{-1} attibutes to the stretching vibration of C=O groups. The stretching vibration of C=C asigned at 1511 cm^{-1} is assigned the presence of aromatics. The weak bands 700 cm^{-1} attribute to the aromatic components along with C-H bending (Liu and Sun 2011; Varma et al. 2019). The FTIR spectrum of PANI@SD biocomposite depicts peaks at 1595 cm^{-1} and 1493 cm^{-1} ascribing to the typical C=C stretching of quinoid and benzenoid rings, respectively. The occurrence of these two bands indicates the synthesis of PANI and the presence of its amine and imine groups (Joubert et al. 2010). The band at 1306 cm^{-1} corresponds to the N-H bending mode. The peak at 822 cm^{-1} could be attributed to the C-H bending in the benzene ring of PANI@SD. The degree of electron delocalization in the quinoid ring of PANI@SD is disclosed by the strong peak around 1145 cm^{-1}. The absorption band asigned at 624 cm^{-1} is associated with the valence vibration of the C-C bond (Imgharn et al. 2021). These findings provide qualitative information by disclosing the deposition of PANI on the sawdust surface. The FTIR spectrum of biobeads displayed peaks around 1087, 1515, 2925, and 3420 cm^{-1} which are ascribed to the tensile vibrations of -COH and -COO- (symmetric), C-H bond relates to the functional group of alkenes and O-H stretching, respectively (Javanbakht and Shafiei 2020). These results show that the beads of the alginate /Ca^{2+} layer were coated with the PANI@SD particles.

3.2. Adsorption study

3.2.1. Influence of adsorbent dosage and Effect of initial pH

To clear up the adsorption process, it is crucial to investigate the parameters influencing the adsorbate-adsorbent interface. The adsorbent dose effect of Alg-PANI@SD biobeads on the removal of OG dyestuff was studied and presented in Fig. 3. From the Fig. 3, it is obvious that the OG dye adsorption efficiency depends on the amount of Alg-PANI@SD biobeads. The percentage of OG dye removal increases as the adsorbent dosage ratio (from 0.5 to 4 g L^{-1}) increases, which is due to the raise in the amount of available binding sites (Liu and Sun 2011; Zheng et al. 2019). The maximum OG dye removal efficiency value of 86.31% was reached for an Alg-PANI@SD dose of 2.5 g L^{-1}. Above 2.5 g L^{-1}, the number of active sites was competent to approximately remove the OG dye from the medium, thereby reflecting irrelevant changes in OG dye adsorption percentage. This removal trend could be elucidated by the overlapping of active sites generated by the congregating of adsorbent particles under high Alg-PANI@SD dosage conditions. Thus, 2.5 g L^{-1} is applied as the optimal adsoebent dose for further adsorption tests.

The pH of solution is a crucial that acts on the adsorption ability by altering the surface capability of the adsorbent and the existing form of adsorbate (Yeamin et al. 2021; Ait Haki et al. 2021). The PZC and the solution pH effect on the adsorption of the OG dye on Alg-PANI @ SD were studied in the pH range from 2 to 10 and illustrated in Fig. 3**(b-c)**, respectively. The PZC point was found to be 5.5, this finding means that the Alg-PANI@SD biobeads surface charged positively at pH values less than the PZC point (pH<PZC) and vice versa. Mainly, the maximum OG dye removal efficiency (94.7%) was reached at pH=2. As far, the OG dye removal favorability at pH<PZC could be suggested as the result of electrostatic attractions between sulfonate groups ($-SO_3Na$)-containing-OG molecules and the Alg-PANI@SD biobeads surface. However, at pH values above the PZC value, the removal of the OG dye gradually decreases as pH increases. This lower affinity for the OG dye may be related to repellency forces. In addition, the pH value 5.0 was selected as an optimal value for further adsorption experiments.

3.2.2. Effect of interfering ions

To figure out the proportional aspects of various competing ions on sulfonate groups ($-SO_3Na$)-containing OG adsorption on Alg-PANI@SD biobeads, the influence of co-existing Cl^-, SO_4^{2-}, CO_3^{2-} and NO_3^- interfering ions were assessed at initial concentrations (100mg L^{-1}) (Abdellaoui et al. 2021). Fig. 4 depicts the interfering ions effect on the OG dye removal percentage by Alg-PANI@SD biobeads. It was assigned that the elimination of OG dye was not influenced by the presence of SO_4^{2-}, Cl^- and NO_3^- ions. In contrast, the presence of CO_3^{2-} ions affects the removal efficiency of OG dye. This carbonate competing trend could be attributed to the producing of hydroxide ions by hydrolysis, which in turn contest for SO_3Na-containing OG binding sites or decrease the solution acidity (Vickers 2017).

3.2.3. Adsorption kinetics

The adsorption kinetic of OG dye onto Alg-PANI@SD biobeads was performed to investigate the relationship between contact time and adsorption capacity for insight into the OG molecule's adsorption process and to provide relevant conditions for the efficient application of Alg-PANI@SD biobeads adsorbent (Mahi et al. 2021). As can be seen in Fig. 5, the OG dye starts to adsorb rapidly onto Alg-

PANI@SD biobeads within the first contact hour owing to the availability of OG adsorption vacant sites. Thereafter, the OG dye removal rate becomes slower until attaining the equilibrium adsorption after 180 min, as a result of the reduction in the number of sulfonate groups ($-SO_3Na$)-containing OG dye-binding sites. Pseudo-first-order (PFO) and pseudo second-order (PSO) kinetic models were empolyed to assess the reaction kinetics (Zheng et al. 2012; Amjlef et al. 2021). The nonlinear expressions and the fitting parameters data of PFO and PSO kinetic models are presented in Table 1 and Fig. 5**(a).** The correlation coefficient (R^2) values indicate that the PFO model (R^2=0.996) is more favorable than the PSO one (R^2=0.995) for OG dye removal on Alg-PANI@SD biobeads. Furthermore, the adsorption capacity, calculated from the PFO model (4.468 mg g^{-1}), was found to be close to the experimentally-determined one (4.301 mg g^{-1}), confirming that the OG dye adsorption process was better described by this kinetic model.

Table 1
Parameters of PFO and PSO models for OG removal onto Alg-PANI@SD from aqueous medium.

$Q_{e.exp}$ (mg.g^{-1})	PFO model $Q_t = Q_e(1 - \exp(-k_{PSO}t))$			PSO model $Q_t = \frac{Q_e^2 k_{PSO} t}{1 + Q_e k_{PSO} t}$		
	k_1	$Q_{e.1}$	R^2	k_2	$Q_{e.2}$	R^2
4.301	0.0157	4.468	0.996	0.0025	5.799	0.995

3.2.4. Adsorption equilibrium

The equilibrium adsorption isotherm is indispensable to figure out the distribution of OG dye molecules at the Alg-PANI@SD surface, when the adsorption gets to the equilibrium (Feng et al. 2020). Therefore, the analysis by Langmuir and Freundlich isothermal models was carried out (Salam et al. 2017), their nonlinear equations and equilibrium data were displayed in Table 2, and their fitting curves are plotting in Fig. 5**(b)**. According to the correlation values, this figure discloses that the OG dye removal onto the Alg-PANI@SD biobeads, was well fitted with the Freundlich model (R^2 =0.991), more than the Langmuir one (R^2 =0.949). This assumes that the OG dye removal onto the heterogeneous as-synthesized biobeads surface was carried out in multilayer.

Table 2
Nonlinear fitting parameters of Langmuir and Freundlich models for OG adsorption on the Alg-PANI@SD biobeads.

Q_{exp}	Langmuir			Freundlich		
($mg.g^{-1}$)	$Q_e = \frac{Q_{max}K_LC_e}{1+K_LC_e}$			$Q_e = K_FC_e^{1/n}$		
	Q_{max} ($mg.g^{-1}$)	K_L ($L.mg^{-1}$)	R^2	n_f	K_F ($mg.g^{-1}$)	R^2
8.03	7.42	0.807	0.949	4.807	3.746	0.991

Conclusion

In this current paper, Alg-PANI@SD biobeads were prepared and applied as were efficient adsorbent to remove OG dyestuff from the aqueous phase. The adsorbent was characterized for the analysis of the surface properties. It was concluded that OG adsorption was affected by several operating factors like adsorbent dosage, pH, contact time and initial OG dye concentration. The adsorption equilibrium was achieved within 180 min at pH 5.0. The OG dye adsorption process on the Alg-PANI@SD biobeads was followed by pseudo-first order kinetics. The isotherm modeling revealed an appropriate fitting of the Freundlich isotherm. The electrostatic interactions between sulfonate groups ($-SO_3Na$)-containing OG dye molecules and Alg-PANI@SD biobeads surface played a primordial role in the adsorption prcocess. In view of the strong adsorption ability of the adsorbent Alg-PANI@SD biobeads over OG dye, easy separability, the present study submits that Alg-PANI@SD biobeads is a novel, effective, and economically feasible for the adsorption of dyes from wastewater containing OG dyestuff.

Declarations

Ethics approval

This study was approved by the research ethics committee of Ibn zohr university.

Consent to participate

All the authors participed in this article

Consent for publication

All the authors agreed this article be published.

Authors Contributions

Abdelaziz Imgharn: Conceptualization, Methodology, Formal analysis, Investigation, Data curation, Writing-original draft. **Nouh Aarab:** Participation in the design. **Abdelghani Hsini**: Writing - review & editing, Investigation, Methodology. **Yassine Naciri**: Writing - review & editing, Investigation, Methodology. **Mahmoud Elhoudi**: Investigation, Methodology. **Mohamed Ait Haki:** Writing - review & editing. **Mohamed Laabd:** Conceptualization, Validation, Writing - review & editing, Investigation, Methodology. **Rajae Lakhmiri**: Supervision. **Abdallah Albourine**: Conceptualization, Supervision.

Funding

This study was not approved and financially supported.

Competing interests

The authors declare no competing interests.

Availability of data and materials

Data and materials are available.

References

1. Abdellaoui Y, Abou Oualid H, Hsini A, et al (2021) Synthesis of zirconium-modified Merlinoite from fly ash for enhanced removal of phosphate in aqueous medium: Experimental studies supported by Monte Carlo/SA simulations. Chem Eng J 404:126600. https://doi.org/10.1016/j.cej.2020.126600
2. Ait Haki M, Imgharn A, Aarab N, et al (2021) Efficient removal of crystal violet dye from aqueous solutions using sodium hydroxide modified avocado shells: kinetics and isotherms modeling. Water Sci Technol wst2021451. https://doi.org/10.2166/wst.2021.451
3. Amjlef A, Khrach S, Ait El Fakir A, et al (2021) Adsorptive properties investigation of natural sand as adsorbent for methylene blue removal from contaminated water. Nanotechnol Environ Eng 6:26. https://doi.org/10.1007/s41204-021-00119-y
4. Chang X, Li M, Liu Q, et al (2016) Adsorption–reduction of chromium(vi) from aqueous solution by phenol–formaldehyde resin microspheres. RSC Adv 6:46879–46888. https://doi.org/10.1039/C6RA07239A
5. Dąbrowski A, Podkościelny P, Hubicki Z, Barczak M (2005) Adsorption of phenolic compounds by activated carbon—a critical review. Chemosphere 58:1049–1070. https://doi.org/10.1016/j.chemosphere.2004.09.067
6. El-Gaayda J, Titchou FE, Oukhrib R, et al (2021) Natural flocculants for the treatment of wastewaters containing dyes or heavy metals: A state-of-the-art review. J Environ Chem Eng 9:106060.

https://doi.org/10.1016/j.jece.2021.106060

7. Essekri A, Hsini A, Naciri Y, et al (2021) Novel citric acid-functionalized brown algae with a high removal efficiency of crystal violet dye from colored wastewaters: insights into equilibrium, adsorption mechanism, and reusability. Int J Phytoremediation 23:336–346. https://doi.org/10.1080/15226514.2020.1813686
8. Feng T, Bavumiragira JP, Wambui MA, et al (2020) Hierarchical porous induced competent removal of low concentration azo dye molecules by generating a leachy crystalline structure H-MIL-53(Fe). Chin Chem Lett 31:2717–2720. https://doi.org/10.1016/j.cclet.2020.04.044
9. Grzegorzek M, Majewska-Nowak K, Ahmed AE (2020) Removal of fluoride from multicomponent water solutions with the use of monovalent selective ion-exchange membranes. Sci Total Environ 722:137681. https://doi.org/10.1016/j.scitotenv.2020.137681
10. Hsini A, Benafqir M, Naciri Y, et al (2021a) Synthesis of an arginine-functionalized polyaniline@FeOOH composite with high removal performance of hexavalent chromium ions from water: Adsorption behavior, regeneration and process capability studies. Colloids Surf Physicochem Eng Asp 617:126274. https://doi.org/10.1016/j.colsurfa.2021.126274
11. Hsini A, Naciri Y, Laabd M, et al (2021b) Development of a novel PANI@WO3 hybrid composite and its application as a promising adsorbent for Cr(VI) ions removal. J Environ Chem Eng 9:105885. https://doi.org/10.1016/j.jece.2021.105885
12. Hsini A, Naciri Y, Laabd M, et al (2020) Synthesis and characterization of arginine-doped polyaniline/walnut shell hybrid composite with superior clean-up ability for chromium (VI) from aqueous media: Equilibrium, reusability and process optimization. J Mol Liq 316:113832. https://doi.org/10.1016/j.molliq.2020.113832
13. Imgharn A, ighnih H, Hsini A, et al (2021) Synthesis and characterization of polyaniline-based biocomposites and their application for effective removal of Orange G dye using adsorption in dynamic regime. Chem Phys Lett 778:138811. https://doi.org/10.1016/j.cplett.2021.138811
14. Javanbakht V, Shafiei R (2020) Preparation and performance of alginate/basil seed mucilage biocomposite for removal of eriochrome black T dye from aqueous solution. Int J Biol Macromol 152:990–1001. https://doi.org/10.1016/j.ijbiomac.2019.10.185
15. Joubert M, Bouhadid M, Bégué D, et al (2010) Conducting polyaniline composite: From syntheses in waterborne systems to chemical sensor devices. Polymer 51:1716–1722. https://doi.org/10.1016/j.polymer.2010.01.052
16. Laabd M, Brahmi Y, El Ibrahimi B, et al (2021) A novel mesoporous Hydroxyapatite@Montmorillonite hybrid composite for high-performance removal of emerging Ciprofloxacin antibiotic from water: Integrated experimental and Monte Carlo computational assessment. J Mol Liq 338:116705. https://doi.org/10.1016/j.molliq.2021.116705
17. Laabd M, Imgharn A, Hsini A, et al (2022) Efficient detoxification of Cr(VI)-containing effluents by sequential adsorption and reduction using a novel cysteine-doped PANi@faujasite composite:

Experimental study supported by advanced statistical physics prediction. J Hazard Mater 422:126857. https://doi.org/10.1016/j.jhazmat.2021.126857

18. Liu D, Sun D (2011) Simulation of indigo carmine dye adsorption on polymer doped sawdust in fixed-bed systems. Desalination Water Treat 27:285–293. https://doi.org/10.5004/dwt.2011.2031
19. Mahi O, Khaldi K, Belardja MS, et al (2021) Development of a New Hybrid Adsorbent from Opuntia Ficus Indica NaOH-Activated with PANI-Reinforced and Its Potential Use in Orange-G Dye Removal. J Inorg Organomet Polym Mater 31:2095–2104. https://doi.org/10.1007/s10904-020-01873-3
20. Miklos DB, Remy C, Jekel M, et al (2018) Evaluation of advanced oxidation processes for water and wastewater treatment – A critical review. Water Res 139:118–131. https://doi.org/10.1016/j.watres.2018.03.042
21. Naciri Y, Hsini A, Bouziani A, et al (2021) Photocatalytic oxidation of pollutants in gas-phase via Ag_3PO_4-based semiconductor photocatalysts: Recent progress, new trends, and future perspectives. Crit Rev Environ Sci Technol 1–44. https://doi.org/10.1080/10643389.2021.1877977
22. Pradhan SS, Konwar K, Ghosh TN, et al (2020) Multifunctional Iron oxide embedded reduced graphene oxide as a versatile adsorbent candidate for effectual arsenic and dye removal. Colloid Interface Sci Commun 39:100319. https://doi.org/10.1016/j.colcom.2020.100319
23. Rocher V, Siaugue J-M, Cabuil V, Bee A (2008) Removal of organic dyes by magnetic alginate beads. Water Res 42:1290–1298. https://doi.org/10.1016/j.watres.2007.09.024
24. Salam MA, Kosa SA, Al-Beladi AA (2017) Application of nanoclay for the adsorptive removal of Orange G dye from aqueous solution. J Mol Liq 241:469–477. https://doi.org/10.1016/j.molliq.2017.06.055
25. Shuang C, Li P, Li A, et al (2012) Quaternized magnetic microspheres for the efficient removal of reactive dyes. Water Res 46:4417–4426. https://doi.org/10.1016/j.watres.2012.05.052
26. Singh V, Chauhan P (2009) Structural and optical characterization of CdS nanoparticles prepared by chemical precipitation method. J Phys Chem Solids 70:1074–1079. https://doi.org/10.1016/j.jpcs.2009.05.024
27. Varma AK, Thakur LS, Shankar R, Mondal P (2019) Pyrolysis of wood sawdust: Effects of process parameters on products yield and characterization of products. Waste Manag 89:224–235. https://doi.org/10.1016/j.wasman.2019.04.016
28. Vickers NJ (2017) Animal Communication: When I'm Calling You, Will You Answer Too? Curr Biol 27:R713–R715. https://doi.org/10.1016/j.cub.2017.05.064
29. Yeamin MdB, Islam MdM, Chowdhury A-N, Awual MdR (2021) Efficient encapsulation of toxic dyes from wastewater using several biodegradable natural polymers and their composites. J Clean Prod 291:125920. https://doi.org/10.1016/j.jclepro.2021.125920
30. Zheng X, Zheng H, Zhou Y, et al (2019) Enhanced adsorption of Orange G from aqueous solutions by quaternary ammonium group-rich magnetic nanoparticles. Colloids Surf Physicochem Eng Asp 580:123746. https://doi.org/10.1016/j.colsurfa.2019.123746

31. Zheng Y, Liu Y, Wang A (2012) Kapok Fiber Oriented Polyaniline for Removal of Sulfonated Dyes. Ind Eng Chem Res 51:10079–10087. https://doi.org/10.1021/ie300246m

Figures

Figure 1

SEM images of SD (a), PANI@SD (b), Alg-PANI@SD bioobeads (c). EDS elemental analysis of SD (d), PANI@SD (e) and Alg-PANI@SD biobeads (f).

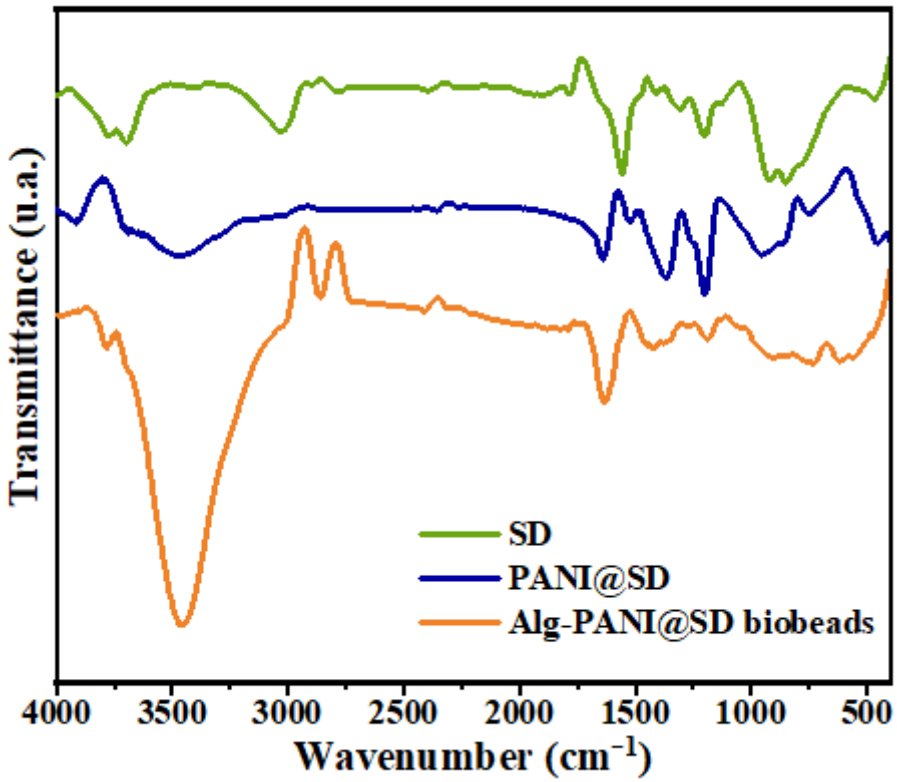

Figure 2

FTIR spectra of SD, PANI@SD and Alg-PANI@SD biobeads.

Figure 3

(a) OG dye adsorption as a function of Alg-PANI@SD biobeads dose (C0 =10 mg L−1, adsorption time = 3 h, T = 298 K and pH = 5.0), (b) initial pH (C0 =10 mg L−1, adsorption time = 3 h, adsorbent concentration = 2.5 g L−1 and T = 298 K), (c) Point of zero charge (pHPZC) of Alg-PANI@SD biobeads.

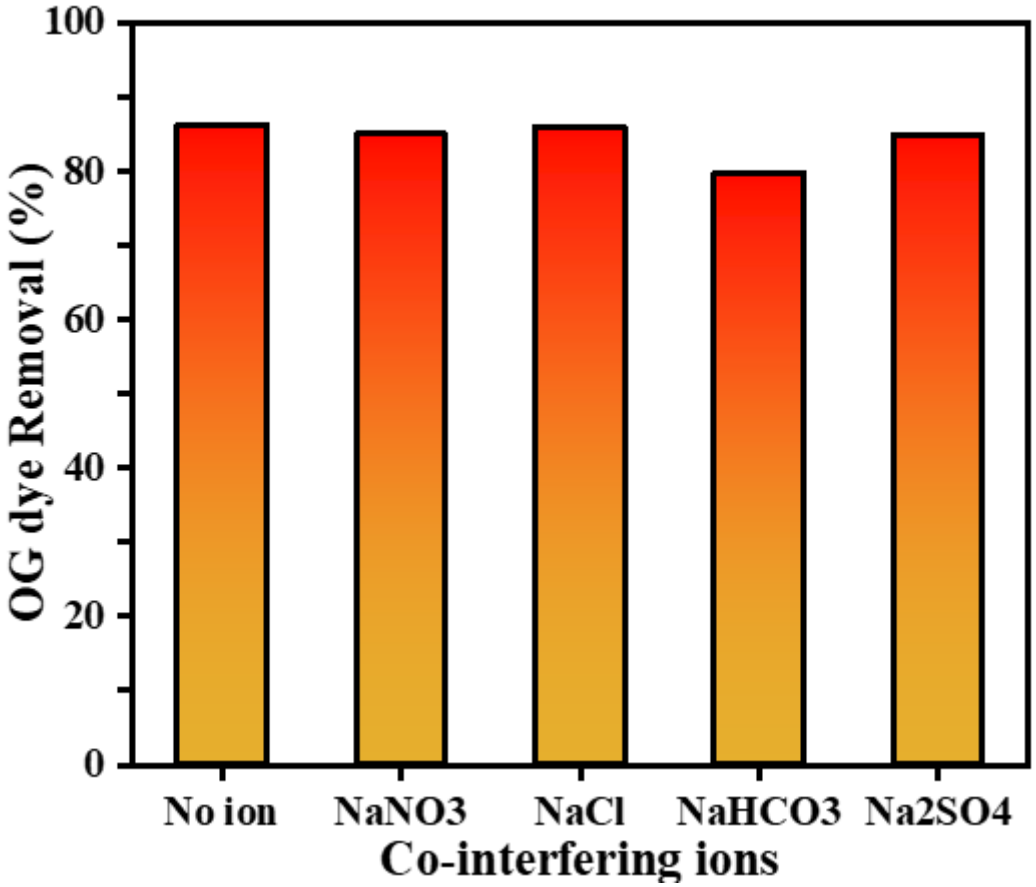

Figure 4

Effect of interfering ions on OG dye removal by Alg-PANI@SD biobeads: adsorbent dose = 2.5 g L-1; pH= 5.0; 10 mg L-1 OG dye concentration; T = 298 K.

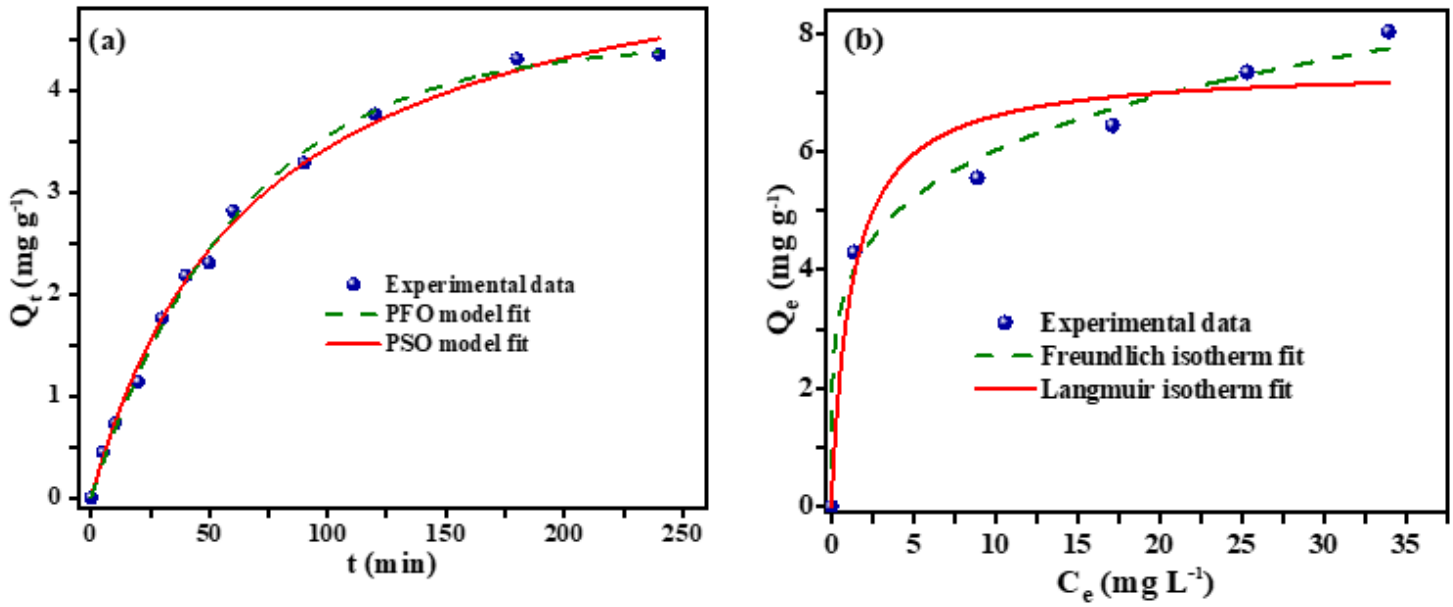

Figure 5

Non-linear PFO, PSO model plots (a), Non-linear Langmuir and Freundlich isotherm plots (b) for the adsorption of OG dye on the Alg-PANI@SD biobeads.